Wood Science and Technology (2020) 54:1529–1549
https://doi.org/10.1007/s00226-020-01237-7

ORIGINAL

Sandwich compression of wood: effect of superheated steam treatment on sandwich compression fixation and its mechanisms

Elin Xiang[1] · Shanghuan Feng[2] · Shumin Yang[3] · Rongfeng Huang[1]

Received: 27 April 2020 / Accepted: 13 October 2020 / Published online: 19 October 2020

Abstract

The permanent fixation is essential for the full industrialization of sandwich-compressed wood. In this study, sandwich-compressed wood was modified with superheated steam for compression fixation. Effects of superheated steam pressure on set-recovery were investigated. Changes in microstructure, chemical structure and cellulose crystalline structure of the compressed wood were analyzed, to clarify the reason and mechanism for sandwich compression fixation under superheated steam treatment. It was found that set-recovery of central-compressed wood was higher than that of surface-compressed wood. Effects of superheated steam treatment on set-recovery were statistically significant ($P < 0.05$). Higher superheated steam pressure contributed to lower set-recovery, but the extent of the impact of superheated steam pressure depended on the pressure levels and the reasons causing the set-recovery (exposure to high humidity, immersion in water or boiling in water). The decreased set-recovery was related to micro-cracks in the cell wall, degradation of hemicelluloses, loss of the C=O linked to the aromatic skeleton in lignin and increase in crystallinity. This research demonstrated that superheated steam treatment is effective in permanently fixing the compression of sandwich-compressed wood.

✉ Rongfeng Huang
huangrf@caf.ac.cn

[1] Research Institute of Wood Industry, Chinese Academy of Forestry, Key Lab of Wood Science and Technology of State Forestry and Grassland Administration, Beijing 100091, People's Republic of China

[2] Research & Development Discovery Center, Zeroignition Technology Inc, Coquitlam, BC V3K 5Z6, Canada

[3] Bamboo and Rattan Science and Technology Laboratory, International Center for Bamboo and Rattan, Beijing 100102, People's Republic of China

Introduction

Wood as a natural porous polymeric material principally consists of cellulose, hemicelluloses and lignin, which are partially crystalline polymer, amorphous linear polymer and amorphous cross-linked polymer, respectively. When the wood cell wall is exposed to polar gases or liquids such as water, ammonia, low molecular alcohols, phenol, amines, it swells. This reduces the elastic modulus and softening temperature of wood; thus, wood plasticity increases (Kaboorani et al. 2013; Morisato et al. 1999; Roszyk et al. 2012). Moreover, wood is constituted of various cells with a hollow structure that provides space for wood compression in loading perpendicular to the fiber axis. Wood sandwich compression technology is a typical instance that applies hydrothermal treatment and compression to wood modification for increased density and enhanced physico-mechanical properties such as stiffness and hardness (Gao et al. 2016, 2018; Li et al. 2018). Traditional wood compression generally refers to the bulk compression, which is achieved by overall pressing at high temperature (higher than 140 °C) after being softened by a hydrothermal treatment (Kutnar et al. 2009; Kitamori et al. 2010). Compared with the traditional wood compression, the positions of compressed layer(s) in wood sandwich compression can be altered to conform to certain specifications if desired, allowing them to be utilized for a variety of applications. On the other hand, since compression occurs only in the compressed layer, wood volume loss is minimized, while the physico-mechanical properties are enhanced.

However, compressed wood without any post-treatment is extremely sensitive to moisture change. When compressed wood without any post-treatment is exposed to liquid or humid environments, the compression can easily recover, known as set-recovery. The dimensional stability of compression wood was not qualified for flooring, furniture and construction uses. To stabilize the properties and quality of compressed wood under changing wood moisture contents, post-treatment is required. Current pathways for wood deformation fixation include resin impregnation (Gabrielli and Kamke 2010; Inoue et al. 1993b), cross-linking reaction (Buchelt et al. 2014; Pfriem et al. 2012), heat treatment (Kutnar and Kamke 2012; Laine et al. 2016; Popescu et al. 2014), etc. Heat treatment has been attracting attention from both academia and industry for wood treatment due to its advantages like low cost, being environmentally friendly and viability for industrialization. Heat treatment at high temperature and saturated steaming of wood can effectively fix wood compression permanently (Laine et al. 2016). It has been reported that when compressed wood is heated at 180 °C and 200 °C, the associated treatment time for permanent compression fixation is 20 h and 5 h, respectively (Inoue et al. 1993a). Saturated steaming of compressed wood can sharply shorten the treatment time for permanent compression fixation. When compressed wood is treated with saturated steam at 165 °C for 30 min, at 180 °C for 8 min or at 200 °C for 2 min, wood set-recovery resulting from boiling in water is lower than 2.0% (Dwianto et al. 1997; Ito et al. 1998; Navi and Heger 2004).

In a previous study, Gao et al. (2019) investigated wood sandwich compression fixation via superheated steam treatment at atmospheric pressure and 0.3 MPa. It

was found that compared with superheated steam treatment at atmospheric pressure, the set-recovery of sandwich-compressed wood with superheated steam treatment at 0.3 MPa was reduced by about 63.8% after moisture absorption and 48.9% after water absorption, respectively. However, the effect of superheated steam treatment on wood sandwich compression fixation and the mechanism is yet to be clarified. In this study, four superheated steam treatment conditions were applied to fix wood sandwich compression. Effects of superheated steam pressure on set-recovery are investigated. Changes in cell-wall microstructure, chemical structure and cellulose crystalline structure of the compressed wood were analyzed, to clarify the reasons and mechanism for sandwich compression fixation under superheated steam treatment.

Materials and methods

Materials

Poplar (*Populus tomentosa*) round wood with a diameter of 25–30 cm and an average air-dry density of 0.44 g/cm^3 was sourced from Guan County, Shandong Province, China. The round wood was processed into lumbers with a dimension of 1000 mm (L)×110 mm (T)×50 mm (R) and then kiln-dried to a moisture content (MC) level of 8.0%. Each lumber was then further processed into two wood lumber samples with a smaller dimension of 400 mm (L)×100 mm (T)×25 mm (R), as illustrated in Fig. 1a.

Sandwich compression

Prior to compression, lumber samples [400 mm (L)×100 mm (T)×25 mm (R)] were firstly coated with paraffin on the transverse sections and then immersed in distilled water at 20 °C for 90 min. As shown in Fig. 1b, each wet sample was cut into two specimens. One was preheated at 165 °C for 10 s for surface-compressed wood; the other one was preheated at 165 °C for 720 s, to make central-compressed wood (as illustrated

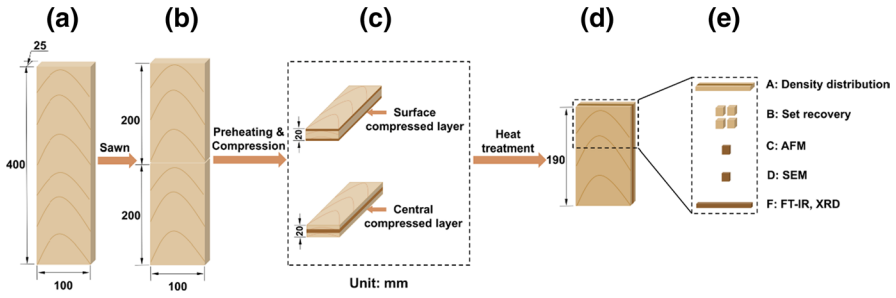

Fig. 1 Schematic diagram of sandwich-compressed wood specimens preparation. Flat-sawn lumber (**a**), wet wood (**b**), sandwich-compressed wood (**c**), sandwich-compressed wood treated with superheated steam (**d**), preparation of test sample (**e**)

in Fig. 1c). After preheating, the specimens were pressed immediately. The detailed compression procedures can be found in Gao et al. (2018) and Li et al. (2018).

Superheated steam treatment of sandwich-compressed wood

The sandwich-compressed wood was firstly oven-dried at 60 °C to a MC level lower than 10% and then treated in a sealed tank (Xinandrying 0938) with superheated steam at 180 °C for 120 min. When the tank temperature rose to 180 °C, a certain amount of water vapor was immediately injected to control the steam pressure of the treatment tank. The superheated steam treatment was conducted at four pressure levels, namely 0.1 MPa, 0.2 MPa, 0.3 MPa and 0.4 MPa, respectively (Fig. 1d). The specific superheated steam treatment procedures are described in a previous study (Gao et al. 2019). During the superheated steam treatment, the samples were placed in the treatment tank at 120 °C, 130 °C and 150 °C, respectively, for 1 h before injecting water vapor to inhibit set-recovery of sandwich-compressed wood (Rautkari and Hughes 2009; Laine et al. 2016). At least three replicates were measured for each treatment condition. The untreated sandwich-compressed specimens were used as control.

Determination of density distribution in sandwich-compressed wood

Prior to compression, one wood specimen with a size of 10 mm (L)×100 mm (T)×25 mm (R) was cut from the original lumber sample for the control wood density determination. After the sandwich compression, another wood specimen with the size of 10 mm (L)×100 mm (T)×20 mm (R) was cut from the area adjacent to the previously cut specimen prior to compression, for the density scanning on the compressed wood. All the cut specimens were exposed to RH 65% at 20 °C for 15 days for conditioning, and then, the density profiles of the specimens were obtained with a soft X-ray densitometer (OFTEX, Japan) with a step of 30 μm.

Determination of set-recovery

To investigate the effect of superheated steam treatment on the set-recovery of sandwich-compressed wood, compressed woods with and without superheated steam treatment were both tested. Cubic specimens with a dimension of 20 mm×20 mm×20 mm were cut from the middle region of the compressed wood for the set-recovery tests. Set-recovery caused by exposure to high humidity, immersion in water and boiling in water was tested at a specified time by the following procedures.

Set-recovery induced by exposure to high humidity

The cubic specimens were exposed to RH 90% at 40 °C. During the exposure, the specimen dimension was tested once a day. After one week of exposure, the specimens were oven-dried at 103 °C to constant weight.

Set-recovery induced by immersion in water

After the tests on set-recovery induced by exposure to high humidity, the specimens were further immersed in water at room temperature and the thickness was tested when the immersion time reached 1 h, 2 h, 3 h, 4 h, 5 h, 6 h, 12 h, 24 h and 48 h, respectively. After 48 h of immersion, the specimen was vacuumed for 1 h and then immersed in water under atmospheric pressure for 6 h, and its thickness was tested again. After 2 days of air-drying, the specimens were oven-dried at 60 °C for 24 h and then further dried at 103 °C to constant weight.

Set-recovery induced by boiling in water

After the tests on set-recovery induced by immersion in water, the specimens were further boiled in water at atmospheric pressure for 2 h, and then, the specimens were air-dried in the laboratory. After 2 days of air-drying, the specimens were oven-dried at 60 °C for 24 h and then further dried at 103 °C to constant weight.

Set-recovery was calculated in accordance with the following Eq. (1):

$$\mathrm{SR} = \frac{d_\mathrm{r} - d_\mathrm{c}}{d_0 - d_\mathrm{c}} \times 100\% \tag{1}$$

where SR (%) is the set-recovery; d_0 (mm) is the thickness of oven-dried wood before compression; d_c (mm) is the thickness of oven-dried wood after compression; d_r (mm) is the thickness of oven-dried wood after exposure to RH 90% at 40 °C for 7 days, after immersion in water, and after boiling in water, respectively.

Data of set-recovery were statistically analyzed via analysis of variance (ANOVA) using the least significant difference method to determine the level of significance at $P < 0.05$.

Characterization of the cell wall of sandwich-compressed wood

Field emission scanning electron microscopy (FESEM)

FESEM was conducted on the compressed layer, transitional layer and uncompressed layer in the sandwich-compressed wood. A thin specimen covering compressed layer, transitional layer and uncompressed layer was cut from the sandwich-compressed wood, and the specimen was firstly air-dried in the laboratory and then further oven-dried at 60 °C for 4 h. The dried specimen was observed by an emission environmental scanning electron microscope (xl-30esem FEG, FEI Company, Hillsboro, OR).

Atomic force microscopy (AFM)

AFM specimens were cut from the sandwich-compressed wood, and the size was 5 mm (L) × 2 mm (T) × 2 mm (R). The specimens were embedded in EPON

812 resin to eliminate the influence of external conditions on the wood cell wall microstructure. After the resin had cured, the transverse surfaces of each specimen were cut with a diamond knife to obtain a smooth transverse surface and then scanned by high-resolution atomic force microscopy (AFM, Veeco, USA). A sharp silicon tip with a nominal radius less than 10 nm was used to image the specimen surface in tapping mode AFM.

Fourier transformed infrared (FTIR)

FTIR specimens were collected from the compressed layer(s) of sandwich-compressed wood. Wood particles were firstly obtained by cutting the compressed layer(s) and then ground to particles to pass a sieve with 200 mesh. After drying at 103 °C for 4 h, the powder was blended with potassium bromide (KBr) and then further manually ground with an agate mortar and made into a test tablet. FTIR tests were carried out with a Nicolet iS10 Fourier transform infrared spectrometer produced by Thermo Nicolet, USA. The spectra were collected for an accumulation of 64 scans with a resolution of 1 cm^{-1} between 4000 and 400 cm^{-1}. OPUS software was used for the baseline correction. The absorption at 1424 cm^{-1}, primarily due to the CH_2 scissor motion in cellulose, was used for spectrum normalization. This absorption band was assumed to be essentially unaltered by the steam treatment (Yin et al. 2011; Guo et al. 2015).

X-ray diffraction (XRD)

To analyze the crystalline structure, sandwich-compressed wood with and without superheated steam treatment was scanned with a X-ray diffractometer (X' Pert-pro30X) using Cu Kα radiation ($\lambda = 0.154$ nm), monochromator (voltage 40 kV, electric current 40 mA) and diffractogram ranges of $2\theta = 5°–40°$ with a scan rate of 3°/min. The crystallinity index (CrI) and crystal dimension were calculated using the Segal method (Segal et al. 1959) and the Scherrer's formula (Wei et al. 2015) as follows:

$$\mathrm{CrI} = \frac{I_{002} - I_{\mathrm{am}}}{I_{002}} \times 100\% \tag{2}$$

$$d = \frac{\lambda}{2 \sin \theta} \tag{3}$$

$$D_{hkl} = \frac{k\lambda}{\beta_{1/2} \cos \theta} \tag{4}$$

where CrI is relative crystallinity (%); I_{002} is the maximum intensity of lattice diffraction angle of 002; I_{am} is the amorphous scattering intensity; D is the width of the crystalline region (nm); d is the crystalline layer spacing (nm); k is the diffraction

constant (0.89); λ is the incident wavelength (0.154); $\beta_{1/2}$ *is* the diffraction peak half wide (radian); θ is the diffraction angle (°).

Results and discussion

Density distribution in sandwich-compressed wood

Figure 2 shows the transverse section images and density distribution in the control wood and sandwich-compressed wood. Surface-compressed wood and central-compressed wood were successfully prepared. When wood was preheated at 165 °C for 10 s, both the top and bottom surfaces are compressed; while when wood was preheated at 165 °C for 720 s, central-compressed wood was obtained (Fig. 2a, b). The relative position was used to compare two specimens with different thickness. For the surface-compressed wood, the thickness and maximum density of the compressed layers is 4 mm and 0.86 g/cm^3, respectively, whereas the density

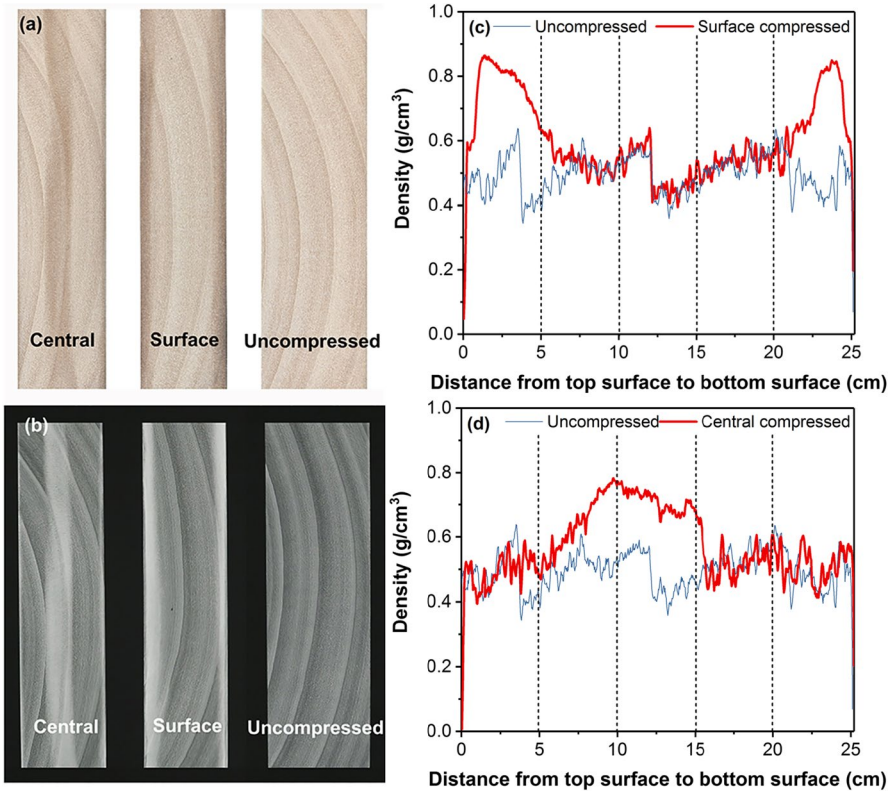

Fig. 2 Photographs (**a**), soft X-ray images (**b**) and density profiles (**c**, **d**) of control wood and sandwich-compressed wood

of uncompressed area in sandwich-compressed wood is almost the same as that of the control wood, confirming that compression only takes place on wood surfaces (Fig. 2c). For the central-compressed wood, the thickness and maximum density of the compressed layer is 8 mm and 0.78 g/cm^3, respectively; the compressed wood surfaces and the uncompressed wood display extremely similar density values (Fig. 2d). These results confirm previous findings that the preheating time can be adjusted to control the density distribution in sandwich-compressed wood (Wu et al. 2019). The effect of superheated steam treatment on the density profile of sandwich-compressed wood has been reported in a previous study (Gao et al. 2019), which demonstrated that superheated steam treatment has no significant impact on the density profile of sandwich-compressed wood. The superheated steam treatment at 0.1 MPa and 0.3 MPa slightly reduced the density profile of sandwich-compressed wood, but no statistically significant difference could be found.

Set-recovery

Figure 3 illustrates the set-recovery of sandwich-compressed wood caused by exposure to high humidity, immersion in water and boiling in water. Set-recovery of central-compressed wood is generally higher than that of surface-compressed wood, and identical superheated steam treatment does not change this phenomenon. However, superheated steam treatment favorably reduces the set-recovery of sandwich-compressed wood, and higher superheated steam pressure contributes to remarkably less set-recovery. This is mainly due to the improvement in the transmission efficiency of superheated steam in sandwich-compressed wood with the increase in steam pressure, thereby accelerating the degradation of amorphous polysaccharides (Ding et al. 2011; Wang et al. 2020). These changes reduce the moisture absorption of wood (Yin et al. 2011), resulting in the reduction in set-recovery of sandwich-compressed wood. For surface-compressed wood and central-compressed wood without superheated steam treatment, the associated set-recovery after exposure to RH 90% at 40 °C for 7 days is 6.40% and 18.36%; immersion of the compressed wood in water leads to increased set-recovery of 47.13% and 65.38%. Boiling of the compressed wood in water further increases the corresponding set-recovery to

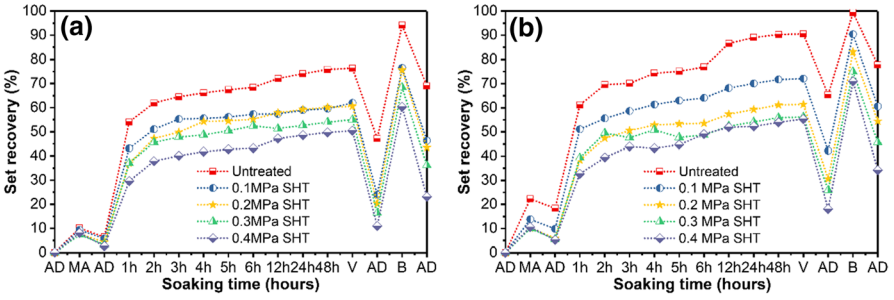

Fig. 3 Set-recovery of sandwich-compressed wood with and without superheated steam treatment. **a** Surface layer compressed wood, **b** central layer compressed wood. *AD* absolute dry, *MA* exposure to high humidity, *V* vacuum, *B* boiling in water, *SHT* superheated steam treatment

69.08% and 80.28%, respectively. Superheated steam treatment of the compressed wood favorably decreases the set-recovery. Superheated steam treatment at 0.1 MPa contributes to a lower set-recovery of 5.75% and 9.84% caused by exposure to high humidity. For surface-compressed wood and central-compressed wood, 0.1 MPa of superheated steam treatment also causes a reduction in set-recovery to 23.90% and 42.19% by immersion in water. While for the set-recovery induced by boiling in water, the set-recovery was reduced from 69.08 and 80.28% to 46.33 and 60.53%, respectively. Increased superheated steam pressure further reduces the set-recovery for both surface-compressed wood and central-compressed wood. When the superheated steam pressure is 0.4 MPa, set-recovery induced by exposure to high humidity decreases to 2.73% and 5.25%, respectively; while for the set-recovery ascribed to boiling in water, the set-recovery is 11.01% and 18.09%, respectively. Furthermore, boiling in water reduces the corresponding set-recovery to 23.02% and 34.13%, respectively. Gao et al. (2019) reported that the pressurized steam treatment was more effective than atmospheric heat treatment in the fixation of compression deformation, which is consistent with the results in this study.

In addition, ANOVA on the set-recovery of sandwich-compressed wood is illustrated in Table 1. F test suggests that superheated steam treatment exerts significant effects on the set-recovery, regardless of the reasons causing the set-recovery, while the extent of the impact of superheated steam pressure on the set-recovery depends on the pressure levels and the reasons causing the set-recovery (exposure to high humidity, immersion in water or boiling in water). For set-recovery caused by exposure to high humidity, superheated steam pressure increases from 0.1 to 0.2 MPa and 0.2 to 0.3 MPa both exert statistically significant differences, while for the

Table 1 Effects of superheated steam on set-recovery of sandwich-compressed wood (values in parentheses are standard deviation)

Testing conditions	Superheated steam treatment	Surface compressed wood		Central compressed wood	
		Average (%)	Difference	Average (%)	Difference
Exposure to high humidity	Untreated	6.40 (0.39)	A	18.36 (2.59)	A
	0.1 MPa SHT	5.75 (0.33)	B	9.84 (0.71)	B
	0.2 MPa SHT	4.29 (0.67)	C	5.98 (0.38)	C
	0.3 MPa SHT	3.29 (0.38)	D	5.49 (0.21)	C
	0.4 MPa SHT	2.73 (0.70)	D	5.25 (0.66)	C
Immersion in water	Untreated	47.13 (1.52)	A	65.38 (4.18)	A
	0.1 MPa SHT	23.90 (2.61)	B	42.19 (4.14)	B
	0.2 MPa SHT	20.20 (2.18)	C	30.52 (3.62)	C
	0.3 MPa SHT	16.42 (2.04)	D	25.88 (2.48)	C
	0.4 MPa SHT	11.01 (1.24)	E	18.09 (2.49)	D
Boiling in water	Untreated	69.08 (2.74)	A	80.28 (1.69)	A
	0.1 MPa SHT	46.33 (3.93)	B	60.53 (1.99)	B
	0.2 MPa SHT	43.46 (3.87)	B	54.40 (3.08)	C
	0.3 MPa SHT	36.19 (2.90)	C	45.62 (3.99	D
	0.4 MPa SHT	23.02 (3.93)	D	34.13 (2.75)	E

central-compressed wood, significant difference is only observed when the pressure increases from 0.1 to 0.2 MPa. For set-recovery caused by immersion in water, each 0.1 MPa increase of the superheated steam pressure in the range of 0.1–0.4 MPa contributes to statistically significant effect on the surface-compressed wood, but for central-compressed wood, a pressure increase from 0.3 to 0.4 MPa does not result in statistically significant difference in the set-recovery. In contrast to the set-recovery induced by immersion in water, set-recovery of central-compressed wood resulting from boiling in water is more sensitive to the superheated steam pressure change. Each 0.1 MPa increase results in statistically significant difference, while for the surface-compressed wood, an increase in superheated steam pressure (from 0.1 to 0.2 MPa) leads to statistically insignificant difference for the set-recovery.

Microstructure

As shown in Fig. 4, sandwich compression results in remarkable deformation of wood vessel and fiber in the compressed layer. Based on the deformation of vessels and fiber on the transverse section with 4 cm width, this area can be divided into three layers: compressed layer (b), transitional layer (c) and uncompressed layer (d). Vessels in the transverse section of the compressed layer are flat (Fig. 4b), vessels in the transitional layer just slightly deform (Fig. 4c), while vessels in the uncompressed layer are almost intact (Fig. 4d). Further observation on the compressed layer at high magnification does not confirm the existence of cell wall buckling, indicating that wood was well softened during the preheating and compressing process (Szcześniak et al. 2008; Wolcott et al. 1990). Microstructure changes in the transverse section of the compressed layer after superheated steam treatment are shown in Fig. 5. In the microscopic analysis, slight separations between compound middle lamella in fiber cells are clearly seen. This is consistent with the results reported by Dogu et al. (2016) on the microstructure changes of thermally compressed poplar wood panels. The cracks of fiber cell wall obviously appeared in superheated steam-treated wood samples.

To eliminate the effects of sample preparation such as blade damage and drying treatment on the crack, AFM was employed to investigate the micro-cracks on the cell wall after superheated steam treatment at higher resolution, and the AFM images are illustrated in Fig. 6. After the compression, negligible micro-cracks are observed on the tension side of the cell wall (Fig. 6a), while folds are observed on the compression side (Fig. 6d). After superheated steam treatment, the fibers in the compressed wood look intact, but the cracks on the cell wall of the superheated steam-treated compressed wood are bigger than that of the untreated compressed wood (Fig. 6b, c, e, f). Micro-crack generally occurs on the S2 layer of the cell wall in the superheated steam-treated compressed wood. When the superheated steam pressure increases from 0.1 to 0.4 MPa, the micro-cracks increase and they gradually propagate from the S3 layer to the S2 layer in cell wall (Fig. 6e, f, white dotted line), forming longer micro-cracks. These cracks may affect the release of the compressive stress, which decreases the set-recovery of sandwich-compressed wood due to moisture absorption or water absorption (Inoue et al. 1993a; Pelit et al. 2016).

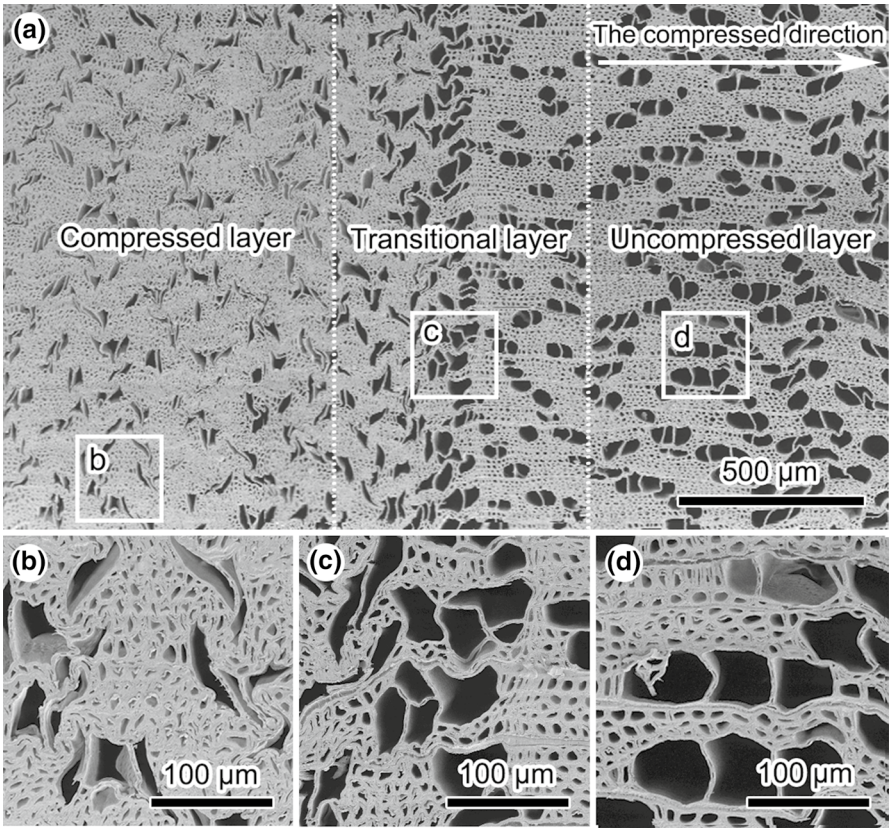

Fig. 4 SEM image of the transverse section of sandwich-compressed wood (**b–d** on the bottom are the SEM image of compressed layer, transitional layer and uncompressed layer with high magnification, respectively)

Therefore, the change in the cell wall microstructure after superheated steam treatment is one of the reasons for the reduced set-recovery.

Microstructure changes on longitudinal surfaces of the compressed wood with and without superheated steam treatment are shown in Fig. 7. For the compressed wood without superheated steam treatment, the lumen of vessels and fibers both buckle and become narrow along the compression direction, and no cracks are observed on the cell wall (Fig. 7a), while for the compressed wood with superheated steam treatment, there is no obvious change in the longitudinal surfaces after 0.1 MPa treatment (Fig. 7b), and a few transverse cracks appeared on the longitudinal surface after 0.4 MPa treatment (Fig. 7c). Figure 7d–f shows the SEM images of pits on the secondary wall of vessels of the compressed wood. For the pits on the secondary wall of vessels of the compressed wood without superheated steam treatment, they are almost intact (Fig. 7d), while cracks along the long axis of the pit membrane are observed on wood vessels of the compressed wood with superheated steam treatment (Fig. 7e, f). These cracks yield more open space in the wood

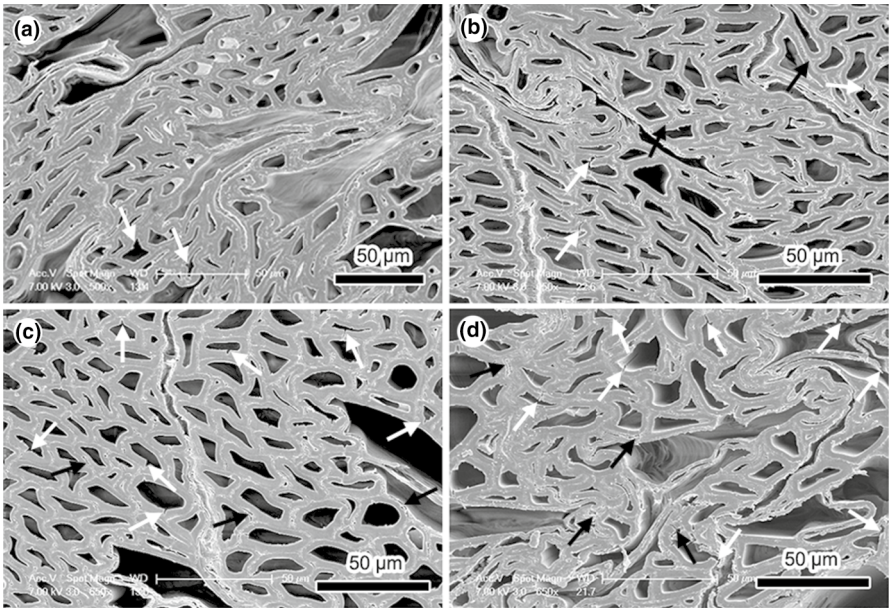

Fig. 5 SEM image of the transverse section of sandwich-compressed wood with superheated steam treatment. Superheated steam treatment at 0.1 MPa **a**, 0.2 MPa **b**, 0.3 MPa **c** and 0.4 MPa **d**, respectively. Separations between compound middle lamella in fiber cells (dark arrow); cracks in fiber cell walls (white arrow)

and thus can further facilitate penetration of superheated steam, which may lead to higher degradation of chemical components (Awoyemi and Jones 2010).

Chemical structure

FTIR spectra of sandwich-compressed wood with and without superheated steam treatment are displayed in Fig. 8. The absorbance intensity varies to a great extent. To further investigate the chemical change attributed to the superheated steam treatment, ratios of the intensity band at 1426 cm^{-1} versus that at 3425 cm^{-1}, 1740 cm^{-1} and 1595 cm^{-1} are calculated and listed in Table 2.

It has been reported that the dimension stability of heat-treated wood is related to the free hydrophilic hydroxyl group (Tjeerdsma and Militz 2005). The IR absorption at 3336 cm^{-1} ascribed to the stretching vibrations of -OH in polysaccharides and lignin decreases with the increased superheated steam pressure. Compared with the surface-compressed wood and central-compressed wood without superheated steam treatment, superheated steam treatment at 0.4 MPa results in the absorbance ratio reduction of 0.31 and 0.26, respectively. Superheated steam treatment at high pressure leads to hemicelluloses degradation into smaller molecules and production of acetic acid. The dehydration polycondensation of cellulose hydroxyls catalyzed by acetic acid results in a remarkable

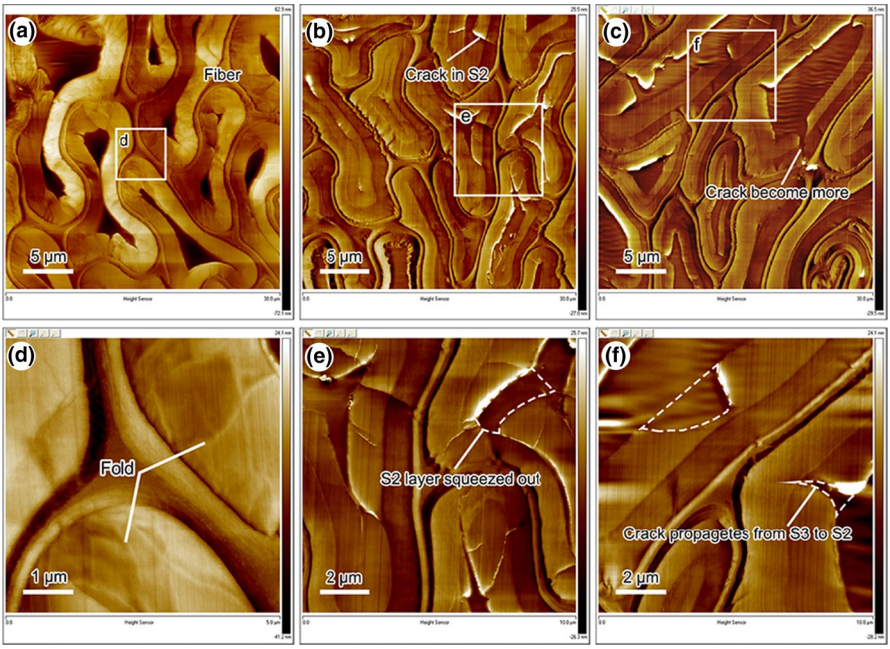

Fig. 6 AFM images on transverse surface of fiber. **a**, **d** Control wood; **b**, **e** superheated steam treatment at 0.1 MPa; **c**, **f** superheated steam treatment at 0.4 MPa

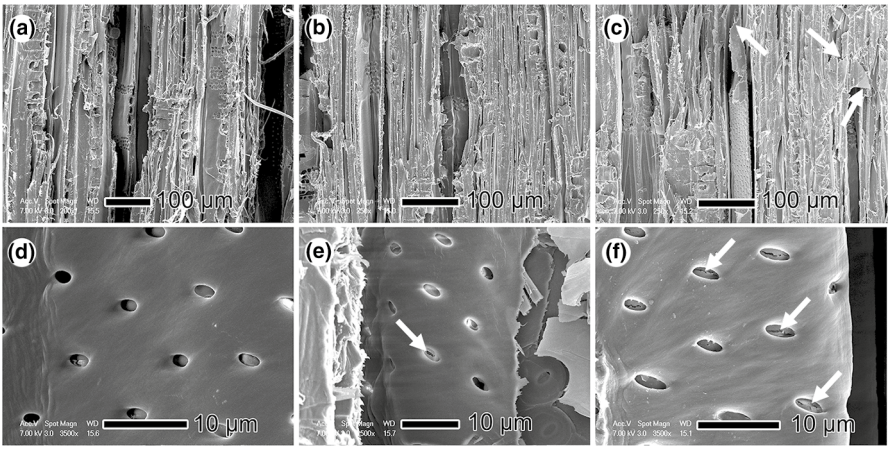

Fig. 7 SEM images on longitudinal surfaces and pits membrane of sandwich-compressed wood with and without superheated steam treatment. **a**, **d** Control; **b**, **e** superheated steam treatment at 0.1 MPa; **c**, **f** superheated steam treatment at 0.4 MPa

reduction in the number of free hydroxyls (Tjeerdsma and Militz 2005; Wang et al. 2020), which is suggested as one of the main reasons for the reduced set-recovery. Absorbance at 1740 cm^{-1} assigned to the C=O stretching vibration

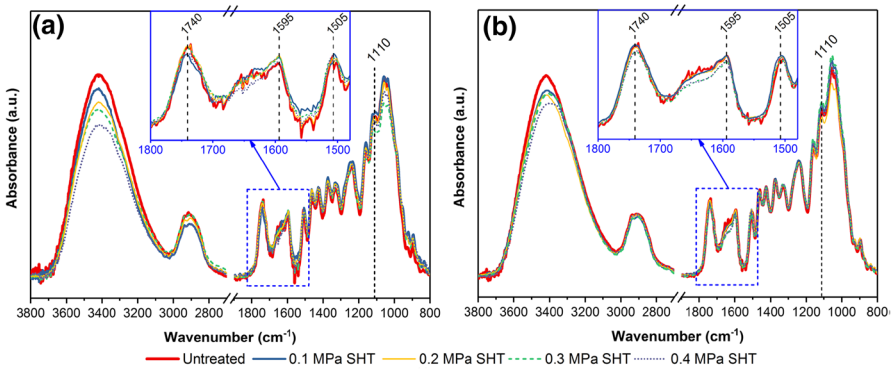

Fig. 8 FTIR spectra of sandwich-compressed wood with and without superheated steam treatment. **a** Surface-compressed wood; **b** central-compressed wood

Table 2 Relative intensity of absorption peak of sandwich-compressed wood before and after superheated steam treatment (values in parentheses are standard deviation)

Sample	Superheated steam treatment	I_{3336}/I_{1426}	I_{1740}/I_{1426}	I_{1595}/I_{1426}
Surface-compressed wood	Untreated	2.18 (0.14)	0.83 (0.02)	0.74 (0.01)
	0.1 MPa SHT	2.11 (0.22)	0.81 (0.02)	0.73 (0.05)
	0.2 MPa SHT	2.02 (0.17)	0.80 (0.06)	0.73 (0.01)
	0.3 MPa SHT	1.97 (0.12)	0.78 (0.03)	0.71 (0.01)
	0.4 MPa SHT	1.87 (0.24)	0.77 (0.05)	0.70 (0.04)
Central-compressed wood	Untreated	2.24 (0.27)	0.86 (0.01)	0.74 (0.02)
	0.1 MPa SHT	2.17 (0.13)	0.84 (0.02)	0.74 (0.01)
	0.2 MPa SHT	2.08 (0.07)	0.82 (0.01)	0.73 (0.01)
	0.3 MPa SHT	2.00 (0.03)	0.80 (0.01)	0.72 (0.02)
	0.4 MPa SHT	1.98 (0.09)	0.78 (0.01)	0.71 (0.01)

in the O=C–OH group of xylan is also lower than that of the compressed wood without superheated steam treatment, which is because of the deacetylation of hemicelluloses (Esteves and Domingos 2013; Guo et al. 2015; Popescu et al. 2011). These degradations reduce the number of hygroscopic sites, resulting in decreased set-recovery. Absorbance at 1595 cm^{-1} is attributed to vibration in the aromatic ring of lignin plus C=O stretching, and superheated steam treatment causes the absorbance reduction, suggesting a loss of the C=O group linked to the aromatic skeleton in lignin during the superheated steam treatment. Superheated steam treatment reduces the absorbance ratio from 0.74 to 0.70 on the surface-compressed wood. For the central-compressed wood, the absorbance ratio reduces from 0.74 to 0.71. The band at 1505 cm^{-1}, which is the characteristic band for C=C stretching of aromatic skeleton vibrations in lignin, increases slightly after superheated steam treatment, indicating the change of lignin in

wood (Guo et al. 2015; Yin et al. 2011). Superheated steam treatment does not lead to remarkable change of C–O related absorbance at 1110 cm^{-1}.

Cellulose crystalline structure

The X-ray diffraction diagrams of sandwich-compressed wood with and without superheated steam treatment are presented in Fig. 9. The obvious diffraction peaks observed at 15.60°, 22.16° and 34.42° are associated with their corresponding crystallographic planes of (101), (002) and (040), respectively (French 2014). The diffractive signal intensity of (002) peak in central-compressed wood treated with superheated steam is slightly higher than that in untreated compressed wood, but this phenomenon is not observed in the surface-compressed wood.

Crystalline parameters such as crystallinity index (CrI), diffraction angles (2θ) and crystalline size are presented in Table 3. The CrI of surface-compressed wood without superheated steam is 39.61%, while the CrI of surface-compressed wood with superheated steam treatments is higher and increases with the increased superheated steam pressure, from 41.59% at 0.1 MPa to 44.26% at 0.4 MPa. A similar change is also observed in the central-compressed wood; the CrI increases from 37.86 to 43.61% when the superheated steam pressure increases from 0.1 to 0.4 MPa. The CrI values of surface-compressed wood are 0.35–2.37% higher than that of central-compressed wood. Temperature is an important factor affecting the crystallinity of wood. When wood is preheated at 165 °C for 10 s to make surface-compressed wood, the surface layer temperature of the wood rose to 150 °C immediately; while when wood is preheated at 165 °C for 720 s for central-compressed wood, the central layer temperature of the wood was 110 °C (Gao 2019). Therefore, the crystallinity of the central-compressed wood is lower than that of the surface-compressed wood. After superheated steam treatment, the CrI values increase due to the increase or reordering in the crystalline region of cellulose (Chen et al. 2018; Tanahashi et al. 1989; Yin et al. 2017).

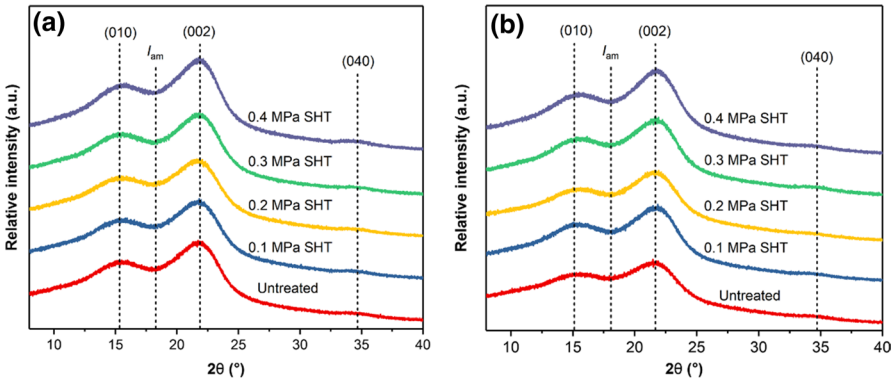

Fig. 9 XRD spectra of sandwich-compressed wood with and without superheated steam treatment. **a** Surface-compressed wood; **b** central-compressed wood

Table 3 Changes in crystalline parameters of sandwich-compressed wood before and after superheated steam treatment (values in parentheses are standard deviation)

Sample	Superheated steam treatment	2θ of (002) plane (°)	Relative crystallinity (CrI, %)	Crystallite thickness (200) of plane (D, nm)	Lattice spacing of (200) plane (d, nm)
Surface-compressed wood	Untreated	21.22 (0.09)	39.61 (2.97)	2.81 (0.06)	0.418
	0.1 MPa SHT	21.29 (0.03)	41.59 (0.75)	3.00 (0.02)	0.417
	0.2 MPa SHT	21.30 (0.06)	42.30 (2.28)	3.04 (0.01)	0.417
	0.3 MPa SHT	21.36 (0.02)	43.63 (1.87)	3.13 (0.07)	0.415
	0.4 MPa SHT	21.39 (0.01)	44.26 (1.18)	3.20 (0.02)	0.415
Central-compressed wood	Untreated	21.17 (0.03)	37.86 (0.41)	2.72 (0.07)	0.419
	0.1 MPa SHT	21.19 (0.01)	39.22 (1.16)	2.92 (0.04)	0.418
	0.2 MPa SHT	21.20 (0.02)	41.35 (0.99)	2.99 (0.01)	0.418
	0.3 MPa SHT	21.26 (0.02)	42.03 (1.83)	3.03 (0.01)	0.417
	0.4 MPa SHT	21.35 (0.03)	43.91 (0.80)	3.09 (0.04)	0.416

The diffraction peaks of (200) slightly shift toward higher 2θ angles when the superheated steam pressure increases, which has also been reported in another study (Kuribayashi et al. 2016). This phenomenon indicates that superheated steam treatment has a clear effect on the crystalline structure of wood cellulose. Higher superheated steam pressure leads to bigger average crystallite thickness. The average crystallite thickness (200) of the surface-compressed wood and central-compressed wood without superheated steam treatment is 2.81 nm and 2.72 nm, respectively. After superheated steam treatment at 0.4 MPa, the average crystallite thickness (200) of the surface-compressed wood and central-compressed wood increases by 17.44% and 13.60%, respectively, to 3.20 nm and 3.09 nm. The increase in crystallite thickness (200) also makes it more difficult for water molecules to penetrate into the interior, further reducing the hydrophilicity of wood (Yin et al. 2011). In contrast, increased superheated steam pressure slightly reduces average lattice spacing (200) by 0.01–0.03 nm for both surfaces of compressed wood and central-compressed wood.

Suggested mechanism for wood sandwich compression fixation with superheated steam treatment

Wood set-recovery can be reduced or even eliminated through the formation of cross-linkages, relaxation of the inner stresses and hydrophobization of cell wall during post-treatment (Chen et al. 2018; Inoue et al. 2008; Navi and Heger 2004). Based on the above analysis and discussion, a mechanism for the wood sandwich compression fixation induced by superheated steam treatment is suggested and illustrated in Fig. 10. Wood cell walls contain several layers. In each layer, cellulose macrostructures cluster along the longitudinal direction to form microfibrils. The microfibrils mix with a matrix consisting of lignin and hemicelluloses (Salmén and Burgert 2009). During superheated steam treatment, deacetylation of hemicelluloses occurs and acetic acid is released (Fig. 10a). The released acetic acid and the pressurized steam further accelerate the degradation of other structural chemical components and thus reduce the number of hydrophilic groups such as hydroxyl and carboxyl leading to a reduction in moisture

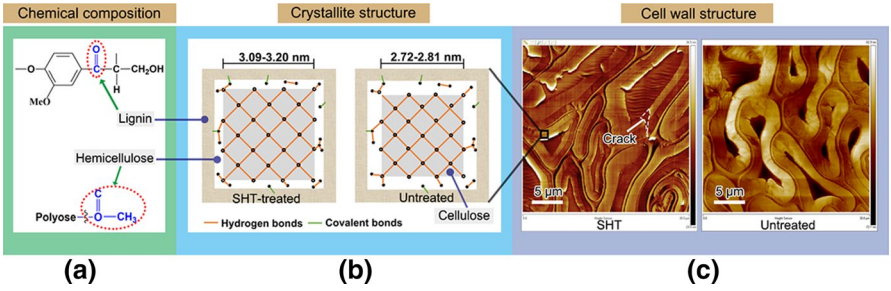

Fig. 10 Suggested mechanism for wood sandwich compression fixation with superheated steam treatment. Change in chemical structure (**a**), cellulose crystalline structure (sketch inspired by Navi and Heger 2004) (**b**) and cell wall structure (**c**) after superheated steam treatment

absorption and water absorption of wood (Li et al. 2017; Tjeerdsma and Militz 2005; Yin et al. 2017). The amorphous hemicelluloses are connected on one side to microfibrils by hydrogen bonds; on the other side, they are linked to lignin by covalent bonds (Navi and Heger 2004) (Fig. 10b). Hemicelluloses degradation also weakens the chemical linkage between microfibrils and lignin, which leads to the reduction in set-recovery due to the relaxation of the internal stresses (Navi and Heger 2004). Due to the rearrangement of cellulose molecules in the adjacent microfibril, cellulose crystallinity and crystallite thickness increase as the steam pressure increases (Fig. 10b). These changes lead to the decrease in the number of adsorption points in cellulose that can be combined with water and further reduce the hydrophilicity of the compressed wood (Guo et al. 2015). In addition, the loss of the C=O group linked to the aromatic skeleton in lignin also results in reduced hygroscopicity (Fig. 10a).

Even though wood cell morphology does not change after superheated steam treatment, cracks on the wood cell wall become more and bigger as the steam pressure increases (Fig. 10c). This can release the compression stress stored in cellulose macromolecule and matrix, further benefiting the compression fixation. These changes in the wood microstructure indicate that the degradation of chemical components in wood is not the only reason for changes in set-recovery during superheated steam treatment. In superheated steam treatment processing, relaxation of the interior stresses and hydrophobization of the cell wall are also responsible for the reduced set-recovery and compression fixation.

Conclusion

Surface-compressed wood and central-compressed wood were successfully prepared via preheating at 165 °C for 10 s and 720 s, respectively. Set-recovery of central-compressed wood was generally higher than that of surface-compressed wood. Superheated steam treatment can significantly reduce the set-recovery of surface-compressed wood and central-compressed wood. Increased superheated steam pressure contributed to reduced set-recovery of sandwich-compressed wood, but the extent of the impact of superheated steam treatment pressure depended on the pressure levels and the reason causing the set-recovery (exposure to high humidity, immersion in water or boiling in water). Chemical structure change during superheated steam treatment, especially the degradation of hemicelluloses, is one of the main reasons for the reduced set-recovery. In addition, micro-cracks formed on the wood cell wall and cellulose crystallinity increase during the superheated steam treatment. Both effects contribute to the compression fixation. With the increase in steam pressure, micro-cracks on the wood cell wall become more and bigger, accelerating the change in the chemical structure. These changes release the compression stress and increase cell wall hydrophobicity, further benefiting the compression fixation. These results indicate that superheated steam treatment process is a potential method to improve the dimensional stability of sandwich-compressed wood.

Acknowledgements The authors acknowledge financial support from the Nature Science Foundation of China (Grant Nos. 31670557; 32071690), and the National Nonprofit Institute Research Grant of CAF (No. CAFYBB2018ZC003).

References

Awoyemi L, Jones IP (2010) Anatomical explanations for the changes in properties of western red cedar (*Thuja plicata*) wood during heat treatment. Wood Sci Technol 45:261–267. https://doi.org/10.1007/s00226-010-0315-9

Buchelt B, Dietrich T, Wagenführ A (2014) Testing of set-recovery of unmodified and furfurylated densified wood by means of water storage and alternating climate tests. Holzforschung 68:23–28. https://doi.org/10.1515/hf-2013-0049

Chen S, Obataya E, Matsuo-Ueda M (2018) Shape fixation of compressed wood by steaming: a mechanism of shape fixation by rearrangement of crystalline cellulose. Wood Sci Technol 52:1229–1241. https://doi.org/10.1007/s00226-018-1026-x

Ding T, Gu L, Liu X (2011) Influenceof steam pressure on chemical changes of heat-treated mongolian pine wood. BioResources 6(2):1880–1889. https://doi.org/10.5552/drind.2011.1106

Dogu D, Davut B, Tuncer D, HizalK CZ (2016) Microscopic investigation of defects in thermally compressed poplar wood panels. Maderas Ciencia Y Tecnologia 18(2):337–348. https://doi.org/10.4067/S0718-221X2016005000031

Dwianto W, Inoue M, Norimoto M (1997) Fixation of compressive deformation of wood by heat treatment. Mokuzai Gakkaishi 43:303–309

Esteves VM, Domingos P (2013) Chemical changes of heat treated pine and eucalypt wood monitored by FTIR. Maderas Cienciay tecnología 15:245–258

French AD (2014) Idealized powder diffraction patterns for cellulose polymorphs. Cellulose 21:885–896. https://doi.org/10.1007/s10570-013-0030-4

Gabrielli CP, Kamke FA (2010) Phenol-formaldehyde impregnation of densified wood for improved dimensional stability. Wood Sci Technol 44:95–104. https://doi.org/10.1007/s00226-009-0253-6

Gao Z (2019) Controllability mechanism and deformation fixation of wood sandwich compression. Beijing Forestry University, Beijing, pp 27–30

Gao Z, Huang R, Lu J, Chen Z, Guo F, Zhan T (2016) Sandwich compression of wood: control of creating density gradient on lumber thickness and properties of compressed wood. Wood Sci Technol 50:833–844. https://doi.org/10.1007/s00226-016-0824-2

Gao Z, Huang R, Chang J, Li R, Wu Y, Wang Y (2018) Sandwich compression of wood: effects of preheating time and moisture distribution on the formation of compressed layer(s). Eur J Wood Prod 77:219–227. https://doi.org/10.1007/s00107-018-1377-x

Gao Z, Huang R, Chang J, Li R, Wu Y (2019) Effects of pressurized superheated-steam heat treatment on set-recovery and mechanical properties of surface-compressed wood. BioResources 14:1718–1730. https://doi.org/10.15376/biores.14.1.1718-1730

Guo J, Song K, Salmén L, Yin Y (2015) Changes of wood cell walls in response to hygro-mechanical steam treatment. Carbohydr Polym 115:207–214. https://doi.org/10.1016/j.carbpol.2014.08.040

Inoue M, Kadokawa N, Nishio J, Misato N (1993a) Permanent fixation of compressive deformation by hygro-thermal treatment using moisture in wood. Wood Res Tech Notes 29:54–61

Inoue M, Ogata S, Kawai S, Rowell RM, Norimoto M (1993b) Fixation of compressed wood using melamine-formaldehyde resin. Wood Fiber Sci 25:404–410

Inoue M, Morooka T, Rowell RM, Norimoto M, Englund F (2008) Mechanism of partial fixation of compressed wood based on a matrix non-softening method. Wood Mat Sci Eng 3:126–130. https://doi.org/10.1080/17480270903020347

Ito Y, Tanahashi M, Shigematsu M, Shinoda Y, Ohta C (1998) Compressive-molding of wood by high-pressure steam-treatment: part 1. development of compressively molded squares from thinnings. Holzforschung 52:211–216. https://doi.org/10.1515/hfsg.1998.52.2.211

Kaboorani A, Blanchet P, Laghdir A (2013) A rapid method to assess viscoelastic and mechanosorptive creep in wood. Wood Fiber Sci 45:370–382

Kitamori A, Jung K, Mori T, Komatsu K (2010) Mechanical properties of compressed wood in accordance with the compression ratio. Mokuzai Gakkaishi 56(2):625–629

Kuribayashi T, Ogawa Y, Rochas C, Matsumoto Y, Heux L, Nishiyama Y (2016) Hydrothermal transformation of wood cellulose crystals into pseudo-orthorhombic structure by cocrystallization. ACS Macro Lett 5:730–734. https://doi.org/10.1021/acsmacrolett.6b00273

Kutnar A, Kamke FA (2012) Influence of temperature and steam environment on set-recovery of compressive deformation of wood. Wood Sci Technol 46:953–964. https://doi.org/10.1007/s00226-011-0456-5

Kutnar A, Kamke FA, Sernek M (2009) Density profile and morphology of viscoelastic thermal compressed wood. Wood Sci Technol 43(1–2):57–68. https://doi.org/10.1007/s00226-008-0198-1

Laine K, Segerholm K, Wålinder M, Rautkari L, Hughes M (2016) Wood densification and thermal modification: hardness, set-recovery and micromorphology. Wood Sci Technol 50:883–894. https://doi.org/10.1007/s00226-016-0835-z

Li T, Cheng D-l, Avramidis S, Wålinder MEP, Zhou D-g (2017) Response of hygroscopicity to heat treatment and its relation to durability of thermally modified wood. Constr Build Mater 144:671–676. https://doi.org/10.1016/j.conbuildmat.2017.03.218

Li R, Gao Z, Feng S, Chang J, Wu Y, Huang R (2018) Effects of preheating temperatures on the formation of sandwich compression and density distribution in the compressed wood. J Wood Sci 64:751–757. https://doi.org/10.1007/s10086-018-1758-0

Morisato K, Hattori A, Ishimaru Y, Urakami H (1999) Adsorption of liquids and swelling of wood V: swelling dependence on the adsorption. Mokuzai Gakkaishi 45:448–454

Navi P, Heger F (2004) Combined densification and thermo-hydro-mechanical processing of wood. MRS Bull 29:332–336. https://doi.org/10.1557/mrs2004.100

Pelit H, Budakçı M, Sönmez A (2016) Effects of heat post-treatment on dimensional stability and water absorption behaviours of mechanically densified Uludağ Fir and black poplar wood. BioResources 11(2):3215–3229. https://doi.org/10.15376/biores.11.2.3215-3229

Pfriem A, Dietrich T, Buchelt B (2012) Furfuryl alcohol impregnation for improved plasticization and fixation during the densification of wood. Holzforschung 66:215–218. https://doi.org/10.1515/hf.2011.134

Popescu M-C, Popescu C-M, Lisa G, Sakata Y (2011) Evaluation of morphological and chemical aspects of different wood species by spectroscopy and thermal methods. J Mol Struct 988:65–72. https://doi.org/10.1016/j.molstruc.2010.12.004

Popescu M-C, Lisa G, Froidevaux J, Navi P, Popescu C-M (2014) Evaluation of the thermal stability and set-recovery of thermo-hydro-mechanically treated lime (*Tilia cordata*) wood. Wood Sci Technol 48:85–97. https://doi.org/10.1007/s00226-013-0588-x

Rautkari L, Hughes M (2009) Eliminating set-recovery in densified wood using a steam heat-treatment proces. In: Processding of the 4th European conference on wood modification. Stockholm

Roszyk E, Mania P, Moliński W (2012) The influence of microfibril angle on creep of Scotch pine wood under tensile stress along the grains. Wood Res 57:347–358

Salmén L, Burgert I (2009) Cell wall features with regard to mechanical performance. A review COST Action E35 2004–2008: wood machining—micromechanics and fracture. Holzforschung 63:121–129. https://doi.org/10.1515/hf.2009.011

Segal LGJMA, Creely JJ, Martin AE (1959) An empirical method for estimating the degree of crystallinity of native cellulose using the X-ray diffractometer. Text Res J 29:786–794. https://doi.org/10.19531/j.issn1001-5299.201809003

Szcześniak L, Rachocki A, Tritt-Goc J (2008) Glass transition temperature and thermal decomposition of cellulose powder. Cellulose 15:445–451. https://doi.org/10.1007/s10570-007-9192-2

Tanahashi M, Goto T, Horii F, Hiral A, Higuchi T (1989) Characterization of steam-exploded wood. iii. Transformation of cellulose crystals and changes of crystallinity. Mokuzai Gakkaishi 34:654–662

Tjeerdsma BF, Militz H (2005) Chemical changes in hydrothermal treated wood: FTIR analysis of combined hydrothermal and dry heat-treated wood. Holz Roh Werkst 63:102–111. https://doi.org/10.1007/s00107-004-0532-8

Wang Q, Wu X, Yuan C, Lou Z, Li Y (2020) Effect of saturated steam heat treatment on physical and chemical properties of bamboo. Molecules 25(1999):1999. https://doi.org/10.3390/molecules25081999

Wei L, McDonald AG, Stark NM (2015) Grafting of bacterial polyhydroxybutyrate (PHB) onto cellulose via in situ reactive extrusion with dicumyl peroxide. Biomacromol 16:1040–1049. https://doi.org/10.1021/acs.biomac.5b00049

Wolcott MP, Kamke FA, Dillard DA (1990) Fundamentals of flakeboard manufacture viscoelastic behavior of the wood component. Wood Fiber Sci 22:345–361

Wu Y, Qin L, Huang R, Gao Z, Li R (2019) Effects of preheating temperature, preheating time and their interaction on the sandwich structure formation and density profile of sandwich-compressed wood. J Wood Sci 65:11. https://doi.org/10.1186/s10086-019-1791-7

Yin Y, Berglund L, Salmén L (2011) Effect of steam treatment on the properties of wood cell walls. Biomacromol 12:194–202. https://doi.org/10.1016/j.molstruc.2010.12.004

Yin J, Yuan T, Lu Y, Song K, Li H, Zhao G, Yin Y (2017) Effect of compression combined with steam treatment on the porosity, chemical compositon and cellulose crystalline structure of wood cell walls. Carbohydr Polym 155:163–172. https://doi.org/10.1016/j.carbpol.2016.08.013